ACTA IMEKO
ISSN: 2221-870X
September 2024, Volume 13, Number 3, 1 - 8

Design of an experimental approach based on the contrast-to-noise ratio measurement for X-ray computed tomography parameters optimization applied to a carbon fiber-reinforced polymer materials scan

Sara Casaccia[1], Giuseppe Pandarese[1], Vincenzo Castorani[2], Gian Marco Revel[1]

[1] *Department of Industrial Engineering and Mathematical Sciences, Università Politecnica delle Marche, Ancona, Italy*
[2] *HP Composites S.p.A., Ascoli piceno, Italy*

ABSTRACT
This paper proposes a systematic approach for the optimization of scan parameters for industrial X-ray computed tomography (XCT), as regard its specific application as diagnostic tool on carbon fiber-reinforced polymer materials (CFRP).
This procedure allows the system operator to overcome suboptimal scan results due to a subjective choice of XCT parameters. In this work, XCT scan quality has been measured in terms of contrast-to-noise ratio (CNR) metric, by calculating it on collected XCT 2D projection images. A four-factor five-level central composite design (CCD) was implemented to perform experiments, and a quadratic polynomial model was chosen to describe the effects of XCT scanning parameters combination on CNR measurement and finally to predict optimal results. Analysis of variance was carried out to evaluate the significance of the model on the response, reporting a R^2 of 97.1 %, and response surface analyses were also performed for CNR optimization purposes. In order to validate the CCD results, different XCT parameters combinations, coming from the CCD analysis on projection images, were used to run different scans, and, as result, the optimal CNR predicted from the model was also reflected in an optimal CNR measured on the reconstructed XCT images.

Section: RESEARCH PAPER

Keywords: X-ray computed tomography; scanning parameters optimization; CFRP materials; CCD model

Citation: S. Casaccia, G. Pandarese, V. Castorani, G. M. Revel, Design of an experimental approach based on the contrast-to-noise ratio measurement for X-ray computed tomography parameters optimization applied to a carbon fiber-reinforced polymer materials scan, Acta IMEKO, vol. 13 (2024) no. 3, pp. 1-8. DOI: 10.21014/actaimeko.v13i3.1789

Section Editor: Laura Fabbiano, Politecnico di Bari, Italy

Received February 21, 2024; **In final form** June 3, 2024; **Published** September 2024

Corresponding author: Sara Casaccia, e-mail: s.casaccia@staff.univpm.it

1. INTRODUCTION

X-ray computed tomography (XCT) is a complex inspection technology, whose usage is spreading on the market other than medical diagnostics [1]. Indeed, in the last decades, it has been widely used in several fields, from aerospace up to automotive, in order to achieve qualitative and quantitative assessments of materials [2].

In particular, the use of XCT as a non-destructive technique on composite materials for automotive industry has increased considerably for its ability to provide detailed information on the internal structure, both in 2D and 3D, and to analyse components from macro and micro-scale point of view.

In detail, as regard composites, XCT is fundamental to study their structural integrity, to detect inner defects occurring during manufacturing or in-service conditions, to understand fiber orientations and to identify porosity [3].

In order to do that, it is clear that one of most relevant aspects to take into account for feature detection is the contrast between the different constituents within the volume of interest, such as matrix, fibres, defects and background.

The XCT image quality depends from the contrast, and this can be reduced due to different factors: artefacts, such as beam hardening, noise, ring effects, or a not sufficient X-rays intensity through the component, made even more complex by heterogeneous materials with not easily distinguishable and in turn similar linear attenuation coefficients.

From this point it is evident the need to set up a careful measurement protocol of XCT parameters in order to optimize

the contrast of the scan and in turn to improve the goodness of a further image processing step [4].

In literature, some works present the relevance of selecting scanning parameters according to the grey values of radiographs to provide suitable penetration of X-rays while minimizing noise [5]. Their main focus was to explain the role of these XCT parameters and their effect on the final scan from a qualitative point of view [5], [6]. Furthermore, other works made use of some commercial software, like ArTist or Scorpius XLab [7], which allow to simulate the result of the XCT scan with certain user-selected parameters, with measurement errors in the order of micrometers for metrological assessment with respect to ground truth geometries.

In our work, the main goal is to develop a quantitative and reliable XCT parameters optimization procedure which can give as result a prediction of the quality of a specific material scan.

The way we achieve our goal was by making use of a Design of Experiment (DOE), which is a branch of applied statistics used for planning and conducting experiments in order to interpret data obtained from them. In particular, we have used it for optimization purpose, by moving the experiments to optimum setting of input variables, which in our case correspond to XCT system parameters [8].

DOE is a robust multipurpose technique which can be used in various situations to identify important experimental factors and to understand the way they are related to a certain response variable.

Khalifa et al. [9] reviewed various DOE methodologies depending on the nature of experimental system and the availability of resources to perform, dwelling on the differences between a full factorial and fractional designs.

Bianchesi et al. [10] described the potential of DOE to find out optimal solution of a response variable through the combination of input variables, according to some algorithms which combine regression model, Ordinary Least Square (OLS) and Analysis of Variance (ANOVA).

The use of OLS to estimate linear regression models, in conjunction with Response Surface Method (RSM), useful to develop, improve and optimize processes, was also discussed in [11], with obtained Mean Square Error (MSE) and determination coefficient (R^2) values of 0.01 and 66.86% respectively, as well as in [12], in which RSM was used to fit a first-order polynomial in the inputs by means of OLS.

Prior research dealt with DOE to improve system performance in many fields of research. Guo et al. [13] indicated the guidelines for conducting DOE to solve chemical processes, suggesting full factorial designs for factors screening, while RSM based on Central Composite Design (CCD) for factors optimization. The use of RSM in analytical chemistry problems was confirmed by Ferreira et al. [14], which performed a multivariate experimental design approach by using a second order model, employing more than two factor levels. Sharif et al. [15] implemented a RSM based on five level-two factor CCD in order to optimize the hydrolysis conditions for maximum ferulic acid production, obtaining an R^2 value of 80.68%. Khazaei et al. [16] identified RSM technique as a valuable tool which facilitated the execution and analysis of experiments in chemistry with respect to the time consuming conventional optimization method which altered one variable at a time by keeping the others constant, without considering the interactive effects between variables, providing a fit with the experimental data of 98.4 %. RSM based on CCD was also preferred in [17], determining optimum operating conditions with a R^2 of 98.6 %, indicating a high reliability of the model in predicting the desired responses.

DOE played an important role in optimization processes also in energy distribution [18], biological [19] and pharmaceutical [20] fields, as well as in material science, in which CCD and RSM are preferred over others DOE approaches for the capability of solving curvature in response associated with each design variable by using quadratic terms.

Our work aims to find out the effect that XCT system parameters have on contrast-to-noise ratio (CNR) value, taken as quality metric of the final performed scan, from a quantitative point of view, that is how this indicator of the XCT scan quality will numerically change according to a certain XCT parameters choice.

A previous study of Portante et al. [21] attempted to overcome the current challenges regarding XCT parameters settings, which involve mainly the biases introduced by operator's ability to run the measurement, instead with DOE based optimization process we achieved an objective and quantitative CNR measurement, independently from the subjective choice of the user. In that work the authors refer to Q-factor calculated on the histogram of reconstructed XCT images of a 3D printed component as a metric of contrast between material and air background, and they identified main factors which could impact the Q-factor responses through a 2-level full factorial DOE. After that, they use RSM to determine the optimal settings. In reverse, our work introduces another way to predict optimal combination of XCT parameters to maximize the contrast of composite materials XCT scan, by performing a specific experimental design based on 2D radiographs, also called projections, created by simply impinging a beam of X-rays through a sample.

This procedure, which represent the greatest novelty compared to the state of the art, will allow to save time and money required for the whole XCT scan process, by providing the operator with a priori knowledge of what will the result of the final XCT scan in terms of contrast.

2. MATERIALS AND METHODS

This section explains the applied procedure in order to choose the optimal XCT parameters for a CFRP scan.

Following a brief overview about the tomographic machine and the material used (Section 2.1), section 2.2 described the type of chosen DOE, which best suited our goal, together with the choice of independent variables and response selection to be involved in our design. Section 2.3 showed how experimental CNR measurements were performed. Section 2.4 outlined the building of the DOE matrix. Subsequently, in Section 2.5, a quadratic multivariate regression model was built according to the design, and through statistical analysis we tried to understand how each variable affected the response. The fit of the model was then evaluated with statistical measurements and residual plots. The combination of XCT parameters to optimize our response variable was identified by using RSM (Section 2.6), from which outliers were removed. Outliers were identified by considering the histogram of projection images, resulting by using certain combination of XCT parameters, and linearity range of detector sensors. The whole procedure was then validated by performing a XCT scan with this parameters' combination, and other three ones, in order to see if the optimal contrast value, calculated from projection images, will reflect in

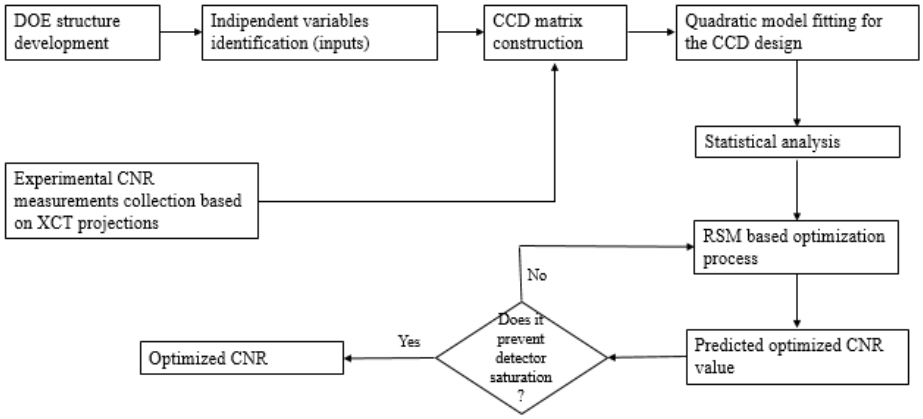

Figure 1. Workflow of the proposed procedure for CNR optimization measurement of XCT scans.

an optimal contrast value even in the reconstructed slices of the scan.

The block diagram (Figure 1) summarizes the workflow.

2.1. Scanned material and X-ray computed tomography system used

All the experimental runs for this study were performed by using a ZEISS Metrotom 1500 laboratory XCT system that has a maximum power output of 200 W (200 kV).

The material considered is a high-strength CFRP (T700 fibres and ER450 epoxy resin) provided by HP Composites S.p.A. company. In particular, the sample under investigation is a cut-out portion of a laminate which was produced by hand lay-up of 6 sheets, oriented at 0°, of a woven carbon fabric prepreg, with a twill 2 × 2 weave pattern and further cured in autoclave (Figure 2, top left). The sample size was 10 × 100 × 3.5 mm³.

2.2. DOE development

In order to find out the optimal combination of XCT scan parameters, a five-level central composite design (CCD) was developed by using Python software. This is a technique widely used to limit the actual number of tests needed through the combination of two-level full factorial design with additional points, also called star points, and two other points taken at the centre of experimental region, fundamental to obtain rotability or orthogonality properties.

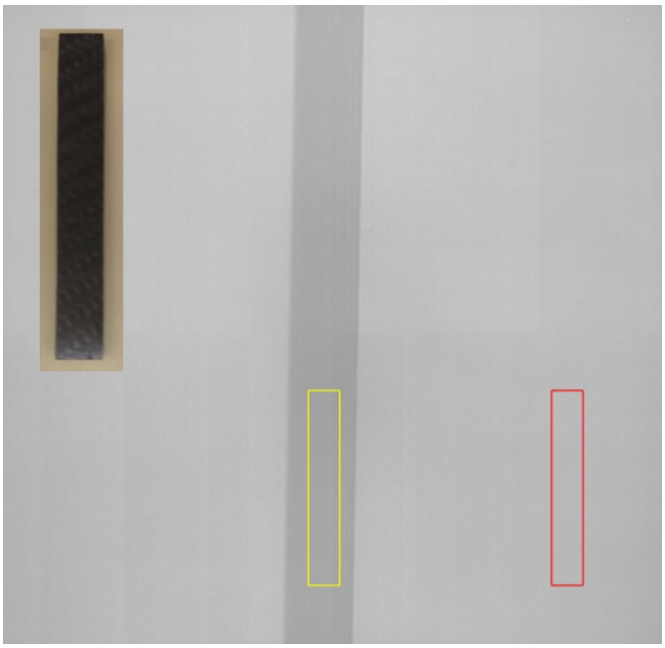

Figure 2. Two ROIs selected on each XCT projection (yellow: material, red: air). On top left a cut-out portion of the investigated material.

The first step performed before building the design matrix was to select independent variables or input factors, together with their numerical range, which could predict the behaviour of a certain response or dependent variable, which will represent our desired outcome.

Since our objective was to optimize the XCT scan of the investigated composite material, from a preliminary analysis the independent variables which affect the XCT scan quality are the voltage (X1), as indicator of the X-ray beam generated power, the beam pre-filter (X2), whose presence could modify the average power of polychromatic X-ray cone beam before impinging the component to be scanned, the exposure time (X3), taken as product of integration time and amount of images averaged in order to reconstruct the XCT image and main index of time duration of XCT final scan, and finally the distance (X4) from X-ray source, which will impact on the maximum achievable XCT spatial resolution since each scan has an acceptable resolution range.

The four selected independent variables were considered at five different levels, coded as –α, -1, 0, 1 and +α.

The α value was calculated using the following formula:

$$\alpha = \left(2^k\right)^{0.25} \tag{1}$$

where k was the number of independent variables, in our study set to 4. Thus, the values of α for this study was set to 2.

The numerical range of these independent variables was selected in a way that the resulting collected X-ray projections did not result in a saturated image, namely the intensity of transmitted X-rays did not overcome the linearity limits of detector sensors, carrying out an uncorrected image.

Moreover, we choose to not consider as input variable the current parameter, since it was calculated by the ZEISS Metrotom 1500 automatically accordingly to the voltage. The link between voltage and current had impact also on the voxel and focal spot size, which in this experiment varied over a range of 7.25 – 17.85 μm.

The gain has been set to 8, since it has been a good compromise to avoid image saturation when the voltage is high and image with low contrast when the voltage is low.

After that, to determine the uncoded value correspondent to α, the following expression was used:

$$UncodedValue = (CoatedValue \cdot L) + C, \tag{2}$$

where coated value was one of the five levels coded values, L was the length expressed in real units between centre points and +1 value of each factor, and C was the centre point expressed in real units.

Table 1 illustrates the input variables used in the design matrix, with their levels coded and correspondent uncoded values.

Table 1. Coded and correspondent uncoded values for independent variables used in DOE matrix.

Indipendent variables	Symbol	-α	-1	0	1	+α
Voltage (kV)	X1	80	100	120	140	160
Filter (mm)	X2	0	0.25	0.5	0.75	1
Exposure time (ms)	X3	2000	4000	6000	8000	10000
Distance (mm)	X4	55	75	95	115	135

2.3. CNR experimental factors determination

After having decided the variables involved and the DOE technique to be used, experimental calculations were made based on projection images. The reference projection image with smallest thickness has been chosen in this paper, since it reported the most unfavourable conditions.

The studied response variable used in this study was the contrast-to-noise ratio (CNR), which provided a quality metric of the XCT scan.

CNR is an important measure in Non-Destructive Techniques (NDT) field and it was used in XCT scan process because it indicates whether the attenuation difference between a feature and its background is greater than background noise level.

The following equation was used to extrapolate CNR value [22], [23]:

$$CNR = \frac{|\mu 1 - \mu 2|}{\sigma 2}, \tag{3}$$

where μ1 and μ2 were the mean grey level intensities calculated on the material and on the background respectively, and σ2 was the standard deviation calculated on the background region to consider the noise level of the image.

Prior assessing the CNR values, XCT projections were exported from METROTOM OS ZEISS software into MATLAB as uint16 tiff images.

Here, a de-striping filtering algorithm [24], based on Wavelet and Fast Fourier analysis, was used to correct vertical stripes inhomogeneities from the raw projections, coming from typical detector measurement errors. This approach resulted in the suppression of just the unwanted structure feasible, while preserving the original image information.

In detail, the original image was Wavelet decomposed up to a certain level L, in order to separate the structural information into horizontal, vertical and diagonal details bands. Then, the bands containing the vertical stripe information were FFT transformed to by a column wise 1D FFT. These coefficients were multiplied with a Gaussian function and then transformed back to the Wavelet space, from which the de-striped image was reconstructed.

To accomplish our goal, three parameters were selected for the filtering process: the highest decomposition level L (set to 3), the Wavelet type (Daubechies, DB30), and the damping factor σ of the Gaussian function (set to 10).

Two Regions of Interest (ROI), shown in Figure 2, were selected corresponding to material (yellow) and air (red) for each collected XCT projection image, and a corresponding CNR value was calculated based on that.

As recommended in [25], minimum number of pixels to consider in order to provide a statistically significant analysis is about 225, and in this work we selected two ROIs with size 97 × 600 pixels, in order to take into account possible hidden defects and artifacts in the projection, which could lead to an alteration of the CNR subsequently calculated.

2.4. CCD matrix

The number (N) of experiments performed to fulfil CCD model was defined by this expression:

$$N = 2^k + 2 \cdot k + C\,, \tag{4}$$

where k is the number of input variables, in our case 4, and C is the number of centre points used (set to 2) in order to check the adequacy of fit and corresponding to a coded value of 0 for each of the independent variables.

Thus, a total of 26 experiments were performed, corresponding to 26 XCT projections on which a CNR was provided.

2.5. Statistical analysis of experimental data

After the CCD matrix was structured and experiments were conducted, the main aim of the study was to find the best combination of factor levels which gives the highest CNR as predicted and optimized response.

A quadratic model fitting was accomplished for the CCD design, and methods like Analysis of Variance (ANOVA) and Ordinary Least Square (OLS) were carried out by means of Python code to evaluate the adequacy of the fitted model, to describe its significance and to study the effects of the variables.

Interactions up to second order were considered, since higher ones were negligible, and the experimental response could be represented by the following equation:

$$Y = \beta_0 + \sum_{i=1}^{k} \beta_i \cdot x_i + \sum_{i=1}^{k} \beta_{ii} \cdot x_{ii}^2 + \sum_{i=1}^{k-1} \sum_{2}^{k} \beta_{ij} \cdot x_i \cdot x_j. \tag{5}$$

Table 2 summarized the effects of the multivariate regression model variables and their associated p value for the response.

By performing OLS and ANOVA, we were able to estimate regression coefficients β_k by minimizing the sum of squares error (SSE). These coefficients represent the mean change in the response variable for unit of change in the predictor variable, while holding other predictors in the model constant.

Table 2. ANOVA and OLS results for the CCD model.

ANOVA and OLS Regression Results			
R^2 = 97.10 %	Adjusted R^2: 93.30 %	F-statistic: 25.98	P-value: $2.12 \cdot 10^{-6}$
	Regression coefficients	***t*-test**	***p*-value**
Intercept	9.38	14.55	0.00
X1	1.68	9.02	0.00
X2	-2.70	-14.53	0.00
X3	0.17	0.91	0.38
X4	1.32	7.11	0.00
X12	-0.51	-2.32	0.04
X22	0.11	0.48	0.64
X32	0.01	0.05	0.96
X42	-0.25	-1.16	0.27
X1*X2	0.64	2.81	0.02
X1*X3	0.03	0.16	0.87
X1*X4	-0.24	-1.07	0.31
X2*X3	-0.03	-0.15	0.88
X2*X4	0.24	1.06	0.31
X3*X4	0.01	0.01	0.99

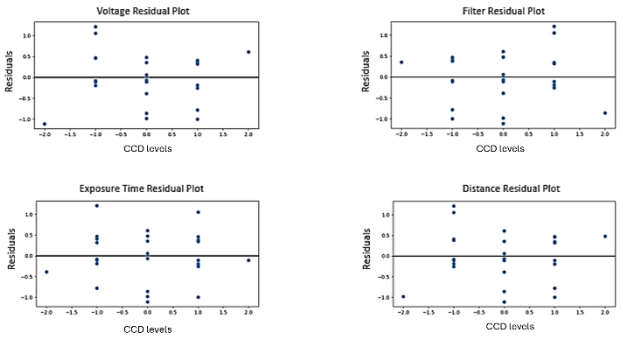

Figure 3. Residual plots for each independent model variable.

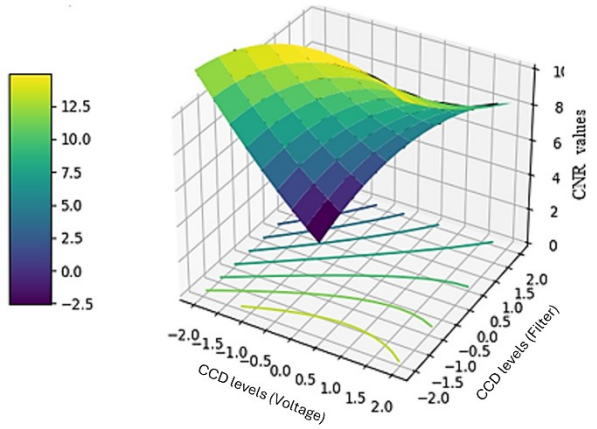

Figure 4. Response surface of the model predicted CNR results by varying voltage and filter and keeping exposure time and distance constant to 0 as coded value.

F-statistic was determined to establish if regression model was statistically significant, at a confidence level of 95%, and to reject the null hypothesis, which expected all regression coefficients equal to 0. A look at t-test also was essential to understand at which extent individual input variables contributed in the prediction of the response.

The determination coefficient (R^2) described how well model predictors, taken as a group, did in predicting the response.

Finally, residual plots (Figure 3) must be considered to validate the model and avoid heteroscedasticity problem with either predictors in the model.

2.6. RSM based optimization process

As mentioned before, the CCD model was used to optimize the XCT measurement process.

In order to identify the optimal factor settings, Response Surface Methodology (RSM) played an important role. Indeed, the response surface is a three-dimensional plot displaying the relationship, based on the quadratic equation shown above, between the response and independent variables. Together with lines of constant response drawn in the plane of the inputs, called contour plot, RSM provided a quick insight of predicted response by the model.

In Figure 4 it could be seen an example of response surface, with the predicted CNR results in function of voltage, filter, exposure time and distance as coded values, by keeping, for instance, the latter two constant to 0.

From the multivariate regression model equation, coordinates of stationary point optimizing the response function could be calculated by solving partial derivatives equation system, given by $\delta Y/\delta X1 = 0$, $\delta Y/\delta X2 = 0$, $\delta Y/\delta X3 = 0$ and $\delta Y/\delta X4 = 0$. This stationary point corresponded to the maximum value of CNR predicted from the response surface (Figure 4).

After having transformed the coded results for XCT parameters combinations into the corresponding uncoded and "real" ones, a further analysis and screening was needed to remove present outliers.

These were given by a list of combinations of XCT parameters which might provide incorrect and unfeasible XCT projection images, being saturated, i.e. in case of voltage values combined with maximum exposure time and distance from X-ray tube.

In order to remove these outliers, a control function was applied.

We considered the dynamic range of our XCT system detector sensors and extracted the linearity limits, which corresponded to 6000 and 55000 in terms of minimum and maximum greyscale level intensities, respectively. We investigated the behaviour of each projection image histogram, and derived from that a control function which provided us the minimum and maximum greyscale values of each image histogram derived from XCT parameters combination and, if it exceeded the fixed linearity limits, caused the corresponding combination to be discarded from the list of those ones resulting from DOE.

In Figure 5 an example of a not saturated projection image (a) and a saturated one (c), together with their histogram (b, d).

3. RESULTS

From RSM analysis, the optimal resulting four XCT parameters combination are those reported on Scan 1 row of Table 3. In order to validate the results obtained, we proceeded to run, for comparison, other three XCT scans (scans 2, 3, 4 from Table 3), gradually changing one variable at a time, starting from voltage (imposing it as an example at 160 kV), followed by exposure time (2000 ms) and finally filter (0.5 mm).

These last three XCT scans parameters combinations were observed to provide a lower CNR value as predicted by RSM.

Afterwards, we considered the reconstructed images from the XCT scan, also called slices, and, after having centered the component with respect to the image center in each of the four scan's slices, we selected two ROIs (Figure 6), having fixed size

Table 3. Scan 1 run with optimal parameters combination from RSM and Scan 2, 3, 4 to validate CCD model results.

Scan number	Voltage (kV)	Current (μA)	Exposure Time (ms)	Gain	Distance from X-ray source (mm)	Focal spot size (μm)	Voxel size (μm)	Magnifi-cation	Filter (mm)	FOV (mm)	Number of slices	Predicted CNR from projections (CCDmodel)
Scan 1	125	129	120	8	115	16	15.85	12.62	0	26 × 23 × 20	1264	15.87
Scan 2	160	99	0.5	8	115	16	15.85	12.62	0	26 × 23 × 20	1259	14.07
Scan 3	160	99	6000	8	115	16	15.85	12.62	0	26 × 23 × 20	1264	13.49
Scan 4	160	99	95	8	115	16	15.85	12.62	0.5	26 × 23 × 20	1267	11.29

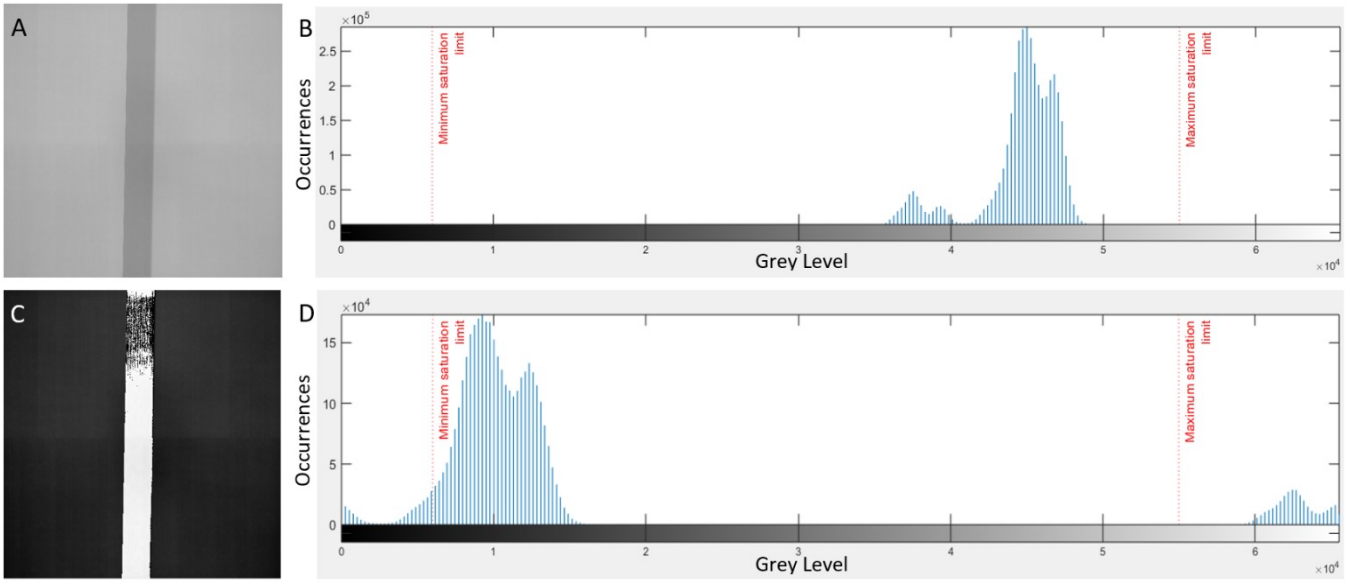

Figure 5. Example of not saturated projection image (A) and a saturated projection (C), together with their respective histograms (B, D).

81 × 511 pixels, one for the material and one for the background, for all slices of the scans.

Subsequently, we used the same CNR formula (Eq.3) as before in order to plot CNR values referring this time to the XCT slices (Figure 7).

In order to further confirm and validate these results, four different projections, one for each scan considered above, were taken into account, and in particular their greyscale level distributions (Figure 8), distinguishing the two different peaks relative to material and air by means of Otsu thresholding (green line).

CNR values based on the projection histogram (here referred as CNR_hist), considering one projection for each of the above four XCT scans, were extracted through the following equation [6]:

$$CNR_{\text{hist}} = \frac{|\mu 2 - \mu 1|}{\sqrt{\sigma 1^2 + \sigma 2^2}}, \tag{6}$$

where μ1 and μ2 are the mean greyscale values for material and air peak respectively, and σ1 and σ2 are the estimated standard deviation of the material and air greyscale values distributions (Figure 9).

4. DISCUSSION AND CONCLUSIONS

The accuracy of the described model can be checked by looking at its determination coefficient R^2, F-statistic results and at the associated residual plot. The former corresponded to 97.1 %, which indicated the percentage of variation in the response explained by the multivariate regression model.

F test turned out to be 25.98, with associated probability value (p-value) of $2.12 \cdot 10^{-6}$, which allowed to state that the developed regression model was statistically significant, meaning that the input variables, taken as a group, predict a significant amount of variance in the response variable.

As regard the residual plot, it fall in a symmetrical pattern in each of the input variables considered in the model, and residuals were centred on zero throughout the range of fitted values. This furtherly guaranteed the model validation.

Signs and values of regression coefficients calculated by OLS and ANOVA represented the influence of predictors on the response, and their associated individual p-value suggested whether or not changes in predictor were associated with changes in the response.

From Table 2, as expected for this kind of investigated material which was not so dense, positive values of regression coefficients for voltage, exposure time and distance exhibited a positive effect on the CNR as response, suggesting that CNR could be slightly improved with the increase of these three settable parameters.

On the other hand, negative value for filter regression coefficient indicated an inverse relationship between this variable and CNR.

In order to locate an optimum set of XCT process parameters, a second order design model based on RSM and fitted with a multivariate quadratic polynomial was fundamental.

Response values for each trial at different factor settings could be predicted by substituting the corresponding values for the

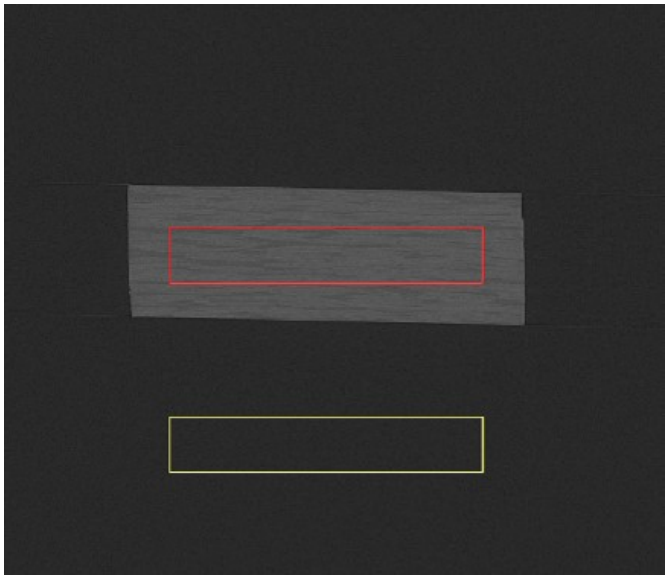

Figure 6. Example of ROIs selection (yellow: air, red: material) on a slice for Scan 1.

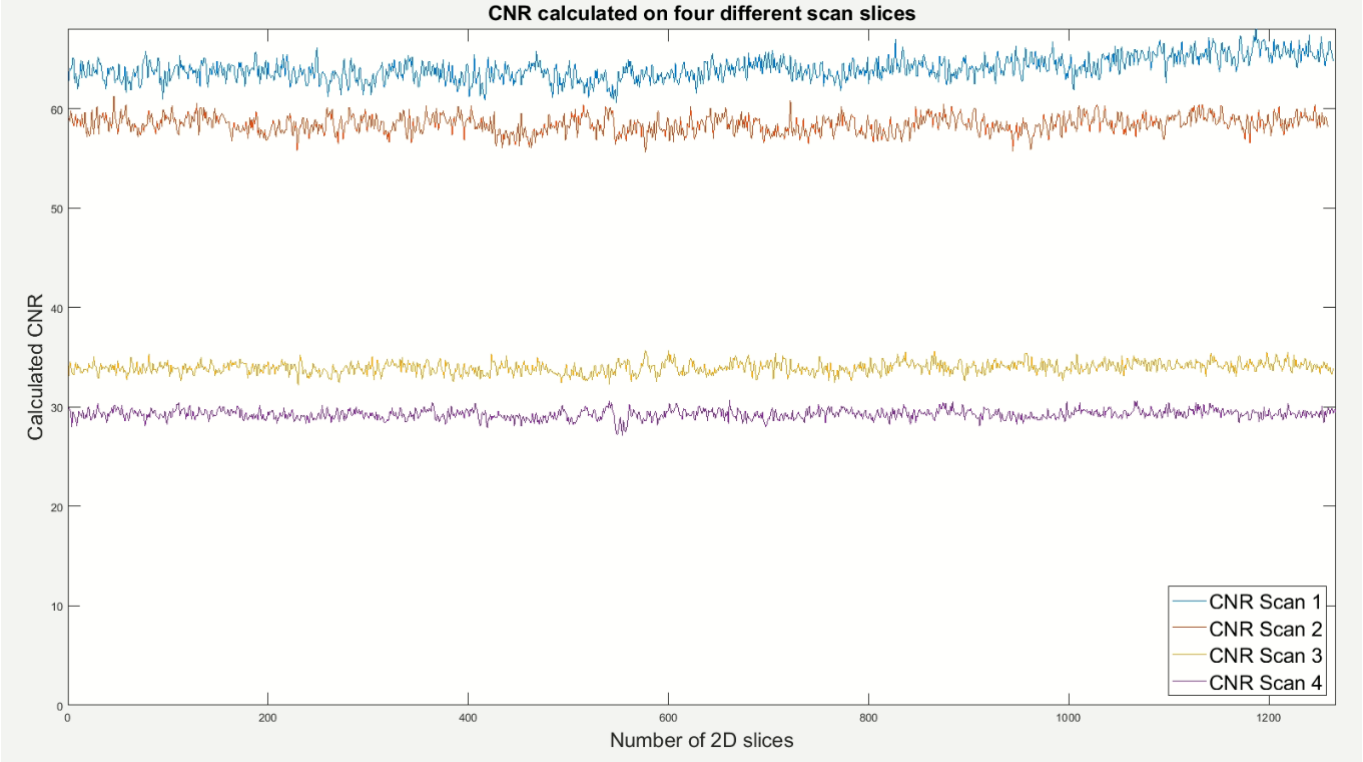

Figure 7. CNR calculated on XCT scan slices.

four factors, four quadratic terms and four 2-factor interaction terms present in the regression equation.

This led to successfully getting the maximum response with the corresponding predictors inside the whole experimental space.

From the RMS results, we took the resulting optimum parameters combination (voltage: 125 kV, filter: 0 mm, exposure time: 6000 ms, distance form X-ray source: 115 mm) and we decided to run a XCT scan with these.

The developed CCD model appears to be reliable, providing high accuracy in predicting CNR values. A prior filtering approach on projection images, based on Wavelet-fft combined algorithm, proved necessary in order to correct images affected by artefacts coming from detector inhomogeneities.

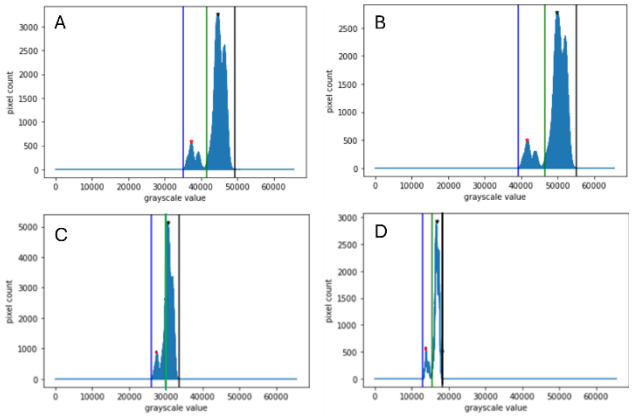

Figure 8. Response surface of the model predicted CNR results by varying voltage and filter and keeping exposure time and distance constant to 0 as coded value. Green line distinguishes two different peaks (material and air), blue and black lines indicate the start and end of the histogram. Red dots indicates the maximum values of the two peaks of the histogram.

In order to validate our CCD model, based on experiments performed on XCT projection images, we launched other three scans taken with a different parameters setting, we calculated CNR values on each scan's reconstructed slices and we compared them.

We obtained CNR measurements which confirmed the goodness of our new proposed approach, with the highest one corresponding to the XCT scan run with the parameters provided by the model.

A second validation was performed by looking at the histogram of these four scans' projections, and also in this case we found out a bigger CNR for the XCT scan launched with the optimal combination of XCT parameters coming from DOE.

In conclusion, many engineering projects involve understanding effects of different predictor variables on a desired output or response.

These experimental-based problems can be challenging, experimental with limited resources.

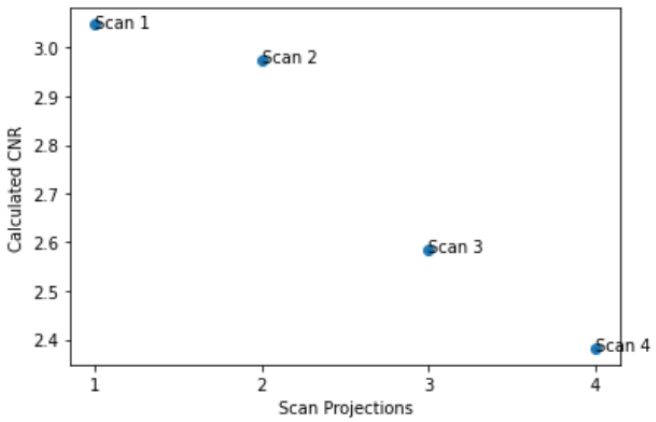

Figure 9. CNR-hist value calculated on each of the four projection.

In this work, we focused on the improvement of the whole XCT measurement process, providing a quantitative result relative to the assessment of scans quality in terms of contrast.

A CCD model development was demonstrated to be useful in order to overcome the lack of knowledge of the correlation between XCT parameters and final scan quality, which governed the XCT process.

Indeed, CCD model allows to provide maximum information with minimum experimental trials and to estimate non linearity of response in a given dataset.

Furthermore, what was highly innovative in our proposed approach was the fact that we collected data from XCT projection images, which allowed the operator not to waste time and money, together with the fact of providing quantitative and objective insights on what would be the outcome of the final XCT scan.

ACKNOWLEDGEMENT

The authors acknowledge HP Composites S.p.A. for providing composite material samples. The XCT system is part of the Laboratorio B+ at DIISM, Università Politecnica delle Marche, funded under the "Dipartimento di eccellenza" program by the Italian Ministry of University and Research.

REFERENCES

[1] S. C. Garcea, Y. Wang, P. J. Withers, X-ray computed tomography of polymer composites, Compos. Sci. Technol. 156 (2018), pp. 305–319.
DOI: 10.1016/j.compscitech.2017.10.023

[2] S. Longo, S. Capuani, F. Granata, F. Neri, E. Fazio, Clinical computed tomography and surface-enhanced Raman scattering characterisation of ancient pigments, Acta IMEKO 10 (2021) 1, pp. 15–22.
DOI: 10.21014/acta_imeko.v10i1.805

[3] A. Trolli, S. Casaccia, G. Pandarese, G. M. Revel, Characterization of porosity and defects on composite materials using X-ray computed tomography and image processing, 8th IEEE Int. Workshop Metrol. Aerosp. MetroAeroSpace, 2021, pp. 479–484.
DOI: 10.1109/MetroAeroSpace51421.2021.9511763

[4] J. Kastner, B. Plank, D. Salaberger, J. Sekelja, Defect and Porosity Determination of Fibre Reinforced Polymers by X-ray Computed Tomography, 2nd Int. Symp. NDT Aerosp., 2010.

[5] M. Reiter, M. Krumm, S. Kasperl, C. Kuhn, M. Erler, D. Weiß, C. Heinzl, C. Gusenbauer, J. Kastner, Evaluation of transmission based image quality optimisation for X-ray computed tomography, Proc. of the Conf. Ind. Comput. Tomogr. iCT 2012, Wels, Austria, 19-21 September 2012.

[6] M. Reiter, D. Weiß, C. Gusenbauer, M. Erler, C. Kuhn, S. Kasperl, J. Kastner, Evaluation of a histogram-based image quality measure for X-ray computed tomography, Proc. of the 5th Conf. Ind. Comput. Tomogr. iCT 2014, Wels, Austria, 25-28 February 2014, pp. 273–282. Online [Accessed 4 September 2024]
https://www.ndt.net/?id=15715

[7] F. Binder, B. A. Bircher, R. Laquai, A. Küng, C. Bellon, F. Meli, A. Deresch, U. Neuschaefer-Rube, T. Hausotte, Methodologies for model parameterization of virtual CTs for measurement uncertainty estimation, Meas. Sci. Technol. 33 (2022), 104002.
DOI: 10.1088/1361-6501/ac7b6a

[8] A. Trolli, S. Casaccia, G. Pandarese, V. Castorani, G. M. Revel, Composite materials characterization based on a computed tomography scan optimization approach, 10th IEEE Int. Workshop Metrol. Aerosp. MetroAeroSpace, 2023, pp. 435–440.
DOI: 10.1109/MetroAeroSpace57412.2023.10189925

[9] O. M. Khalifa, S. A. S. Ali, A. S. Ali, H. Fgaier, A. Elkamel, Using MS Excel to Design and Optimize Response Surface Methodology-Based Engineering Problems, Proc. 5th NA Int. Conf. Ind. Eng. Oper. Manag. Detroit (2020).

[10] N. M. Puggina Bianchesi, E. L. Romão, M. F. B. P. Lopes, P. P. Balestrassi, A. P. De Paiva, A Design of Experiments Comparative Study on Clustering Methods, IEEE Access 7 (2019), pp. 167726–167738.
DOI: 10.1109/access.2019.2953528

[11] S. Basalamah, E. Widodo, Response Surface Model with Comparison of OLS Estimation and MM Estimation, Indones. J. Stat. Its Appl. 5 (2021), pp. 273–283.

[12] J. P. C. Kleijnen, D. den Hertog, E. Angün, Response surface methodology's steepest ascent and step size revisited, Eur. J. Oper. Res. 159 (2004), pp. 121–131.
DOI: 10.1016/s0377-2217(03)00414-4

[13] H. Guo, A. Mettas, Design of experiments and data analysis, in: 2012 Annu. Reliab. Maintainab. Symp., 2010.

[14] S. L. C. Ferreira, W. N. L. dos Santos, C. M. Quintella, B. B. Neto, J. M. Bosque-Sendra, Doehlert matrix: a chemometric tool for analytical chemistry—review, Talanta 63 (2004), pp- 1061–1067.
DOI: 10.1016/j.talanta.2004.01.015

[15] S. N. Ismail, N. Zainol, Optimization of ferulic acid extraction from banana stem waste, Asian J Microbiol Biotechnol Env. Sci 16 (2014) 479–484. ISSN: 0972-3005.

[16] M. Khazaei, S. Nasseri, M. R. Ganjali, M. Khoobi, R. Nabizadeh, A. H. Mahvi, S. Nazmara, E. Gholibegloo, Response surface modeling of lead (II) removal by graphene oxide-Fe3O4 nanocomposite using central composite design, J. Environ. Health Sci. Eng. 14 (2016) 2.
DOI: 10.1186/s40201-016-0243-1

[17] A. E. Sarrai, S. Hanini, N. K. Merzouk, D. Tassalit, T. Szabó, K. Hernádi, L. Nagy, Using Central Composite Experimental Design to Optimize the Degradation of Tylosin from Aqueous Solution by Photo-Fenton Reaction, Materials 9 (2016), 428.
DOI: 10.3390/ma9060428

[18] L. F. S. Caldas, C. E. R. de Paula, D. M. Brum, R. J. Cassella, Application of a four-variables Doehlert design for the multivariate optimization of copper determination in petroleum-derived insulating oils by GFAAS employing the dilute-and-shot approach, Fuel 105 (2013), pp. 503–511.
DOI: 10.1016/j.fuel.2012.10.026

[19] L. Zhang, C. M. Borror, T. R. Sandrin, A Designed Experiments Approach to Optimization of Automated Data Acquisition during Characterization of Bacteria with MALDI-TOF Mass Spectrometry, PLOS ONE 9 (2014), e92720.
DOI: 10.1371/journal.pone.0092720

[20] S. Bhattacharya, Central Composite Design for Response Surface Methodology and Its Application in Pharmacy, in: Response Surf. Methodol. Eng. Sci., IntechOpen, 2021.
DOI: 10.5772/intechopen.95835

[21] E. Portante, A. DeJong, D. Drive, Design of Experiments for Optimal CT Scan Settings of Plastic Components, 8th Conf. Ind. Comput. Tomogr. (2018)

[22] G. Ziółkowski, J. Pach, D. Pyka, T. Kurzynowski, K. Jamroziak, X-ray Computed Tomography for the Development of Ballistic Composite, Materials 13 (2020), 5566.
DOI: 10.3390/ma13235566

[23] G. M. Revel, G. Pandarese, G. Allevi, Quantitative defect size estimation in shearography inspection by wavelet transform and shear correction, IEEE Int. Workshop Metrol. Aerosp. MetroAeroSpace, 2017, pp. 535–540.
DOI: 10.1109/MetroAeroSpace.2017.7999631

[24] B. Münch, P. Trtik, F. Marone, M. Stampanoni, Stripe and ring artifact removal with combined wavelet — Fourier filtering, Opt. Express 17 (2009), pp. 8567–8591.
DOI: 10.1364/oe.17.008567

[25] ASTM International, Standard Test Method for Measurement of Computed Tomography (CT) System Performance, Online [Accessed 4 September 2024]
https://www.astm.org/e1695-20.html